# FEM Analysis of Electric Field Distribution Under Different Material Characteristics in Optical Fiber Insulator

**Wenhao Lu, Jiuhui Zhao, Yanjie Cui, Yang Feng, Liang Liu, Shengtao Li, Wei Xiao, and Senlin Zhao**

**Abstract** Optical fiber current transformer (OFCT) is widely used in flexible DC transmission to improve the ability of information perception of power grid, and optical fiber insulator is the key component of OFCT to provide insulation and protection. However, discharges in optical fiber insulator seriously affect the stable operation of the power system. Here, the effect of material characteristics of different parts on the electric field distribution in insulator is explored to figure out the inner discharge mechanism. A $\pm$ 400 kV optical fiber insulator 3D simulation model is constructed in COMSOL Multiphysics, and differences in the electric field distribution in the insulator are compared and analyzed by finite element method under different conductivity of materials. The results show that the conductivity of the fiber coating and filling compound significantly affects the electric filed at interfaces in the insulator flange sections. The semiconducting fiber coating results in a mismatched potential into the flange sections at both terminals, which further leads to a remarkable electric field distortion on the inner wall of fiber sheath at the interface between the sheath and coating layer. The maximum electric field at the interface is even up to 84.5 kV/mm. The electric field distortion also occurs at the interface between epoxy

W. Lu · Y. Cui
Electric Power Research Institute, CSG EHV Power Transmission Company, Guangzhou 510663, Guangdong, China

J. Zhao · Y. Feng (✉) · S. Li (✉)
State Key Laboratory of Electrical Insulation and Power Equipment, Xi'an Jiaotong University, Xi'an 710049, Shaanxi, China
e-mail: fengyang@xjtu.edu.cn

S. Li
e-mail: sli@mail.xjtu.edu.cn

L. Liu
NR Electric Power Electronics Co., Ltd., Changzhou 213100, Jiangsu, China

W. Xiao
Electric Power Research Institute, CSG, Guangzhou 510663, Guangdong, China

S. Zhao
Nanjing Nari-Relays Electric Co., Ltd, Nangjing 211122, Jiangsu, China



X. Dong and L. Cai (eds.), *The Proceedings of 2023 4th International Symposium on Insulation and Discharge Computation for Power Equipment (IDCOMPU2023)*, Lecture Notes in Electrical Engineering 1102, https://doi.org/10.1007/978-981-99-7405-4_62

tube and filling compound when the conductivity of the filling compound increases. Therefore, the increases in conductivity of the fiber coating and filling compound leads to electric field distortion at interfaces, which can cause discharges in the optical fiber insulator.

**Keywords** Finite element simulation · Electric field · Optical fiber insulator · Conductivity

## 1 Introduction

Flexible high-voltage DC transmission based on modular multilevel converts has a broad application prospect in renewable energy power generation, long-distance power transmission and so on [1–4]. Flexible DC transmission requires higher sampling accuracy, response speed and dynamic range, which makes optical fiber current transformer (OFCT) widely used in various flexible DC transmissions because of its fast response speed and wide measurement range [5, 6].

Kunliulong project is the first ± 800 kV multi-terminal flexible DC transmission project in the whole world [7–10]. However, a large number of optical fiber current transformers failed due to the damage of optical fiber insulators. After carful dissection, it is found that the failure of the optical fiber insulator is derived from the internal discharges, especially at the interfaces between different materials in the metal flanges at high- and low-voltage terminals, which seriously threats the stable operation of the power system.

In order to improve the stability of the OFCT, it is urgent to explore the mechanism of discharges in the optical fiber insulator. In this work, the effect of material characteristics on the electric field distribution in the optical fiber insulator is systematically studied using finite element simulation method. As the conductivities of fiber coating and filling compound change, the fluctuations in the internal electric field distribution characteristics of the insulator are calculated and analyzed. The influence of material conductivity on the electric field distortion is then discussed to figure out the origin of discharges.

## 2 Methodology

### *2.1 3D Simulation Model of Optical Fiber Insulator*

A ± 400 kV optical fiber insulator is utilized to study the effect of material characteristics on the electric field distribution. The 3D simulation model of the insulator is shown in Fig. 1. The optical fiber insulator is composed of silicone rubber shed, epoxy tube, filling compound and optical fiber unit from outside to inside. The optical fiber

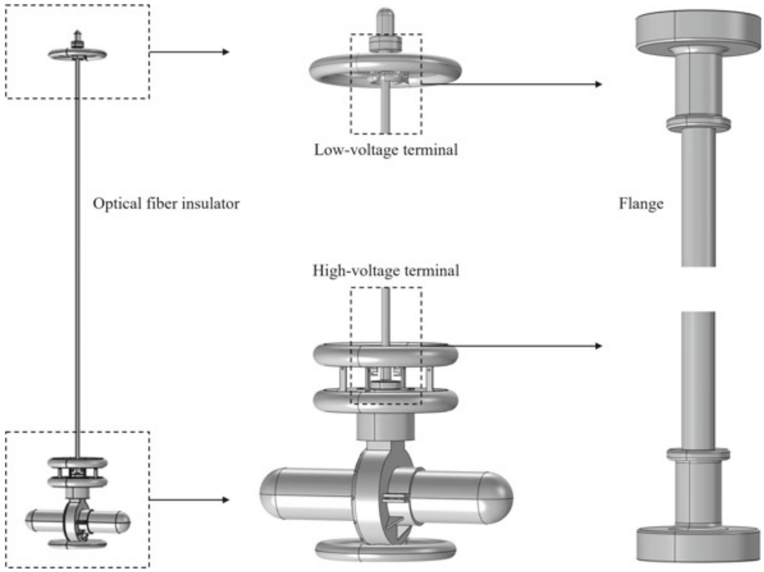


**Fig. 1** 3D simulation model of the optical fiber insulator

**Table 1** Structures and electrical parameters of materials

| Structure | Material | Conductivity (S/m) | Permittivity |
|---|---|---|---|
| Flange | Steel | $1.00 \times 10^{6}$ | 1.00 |
| Shed | Silicone rubber | $3.57 \times 10^{-14}$ | 3.35 |
| Epoxy tube | Epoxy resin | $1.30 \times 10^{-13}$ | 4.92 |
| Filling compound | Multicomponent mixture | $1.00 \times 10^{-13}$ | 2.08 |
| Optical fiber sheath | ETFE | $1.33 \times 10^{-15}$ | 2.48 |
| Coating layer | Semi-conductive coating | $1.25 \times 10^{-9}$ | 36 |
| Optical fiber core | Silica glass | $1.00 \times 10^{-14}$ | 3.75 |

unit consists of the fiber sheath, coating layer and fiber core. Materials and electrical parameters of each structure are shown in Table 1. By dissecting the damaged optical fiber insulator, it is found that the discharge occurs in both high- and low-voltage flange terminals. Given that, our work is focused on the above-mentioned positions.

## 2.2 Calculation Principle

Electric field strength can be calculated from Maxwell's equations. Since the optical fiber insulator is operated under DC voltage, the simplified Maxwell's equations of constant current field are used, which can be expressed as follows,

$$\begin{cases} \nabla \cdot \boldsymbol{J} = Q \\ \boldsymbol{E} = -\nabla V \end{cases} \tag{1}$$

where $\boldsymbol{J}$ is current density vector, $Q$ is quantity of charge, $\boldsymbol{E}$ is electric field strength vector, $V$ is potential.

For isotropic media, the constitutive relations are as follows,

$$\begin{cases} \boldsymbol{J} = \sigma \boldsymbol{E} \\ \boldsymbol{D} = \varepsilon_0 \varepsilon_r \boldsymbol{E} \end{cases} \tag{2}$$

where $\sigma$ is conductivity, $\boldsymbol{D}$ is electric displacement vector, $\varepsilon_0$ is dielectric constant of vacuum, $\varepsilon_r$ is relative dielectric constant of media.

These quantities must obey the principles followed with boundary conditions. The boundary of the simulation domain is electrically insulating, which can be expressed as follows,

$$\boldsymbol{n} \cdot \boldsymbol{J} = 0 \tag{3}$$

where $\boldsymbol{n}$ is normal vector.

Considering the operating conditions of OFCT, the metal flanges at the high-voltage terminal $V_H$ and at the low-voltage terminal $V_L$ are set to 400 kV and 0 kV, respectively.

$$\begin{cases} V_H = 400\,\text{kV} \\ V_L = 0 \end{cases} \tag{4}$$

The geometric model is divided into free tetrahedral mesh cells for 3D finite element calculation based on the above equations and boundary conditions. The electric field distribution is obtained from electric potential by solving the partial differential equation for the three-dimension domain.

# 3 Results and Analysis

## *3.1 Distribution of Potential and Electric Field*

Figure 2 shows the potential distribution at the terminals of the optical fiber insulator. It is found that the potentials on the silicone rubber, epoxy tube and filling compound synchronously increase when gradually approaching the high-voltage terminal. In the flange section, all potentials on these materials remain at 400 kV. However, the voltage in the potential distribution graph shows an obvious difference between the coating layer, fiber core and outlet of the fiber. It inevitably leads to a potential gradient on the fiber sheath. Similarly, the potential of the coating layer and fiber core at the low-voltage terminal in the flange section is higher than that of the outlet parts. It also results in a potential gradient on the fiber sheath in the low-voltage terminal, which further produces a radial electric field strength.

The potentials of the filling compound and coating layer along the axial direction are extracted and shown in Fig. 3. It is found that the electric potentials on the filling compound and the coating layer remain consistent out of the flange sections, while the potential difference between them occurs near and in both flange sections. And the largest potential difference is observed in both flange sections. This is because the semiconducting fiber coating layer exhibits a slower change in potential compared with the insulating filling compound in both flange sections. Therefore, the conductivity of materials in the optical fiber insulator plays an important role in electric potential distribution.

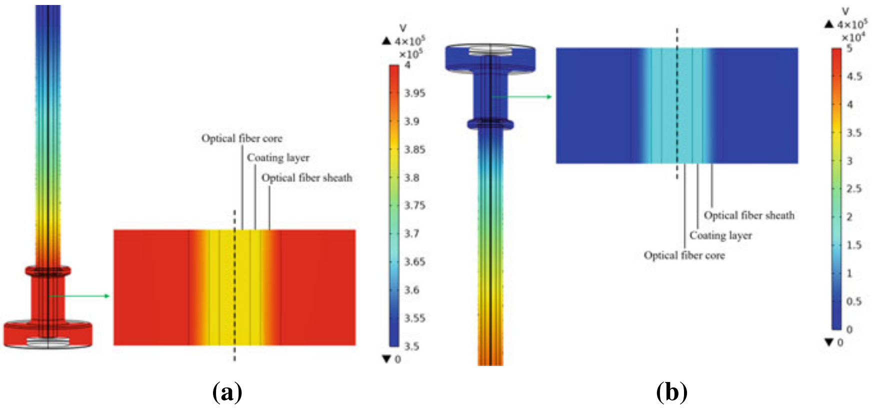


**Fig. 2** Potential distribution at **a** high-voltage terminal and **b** low-voltage terminal

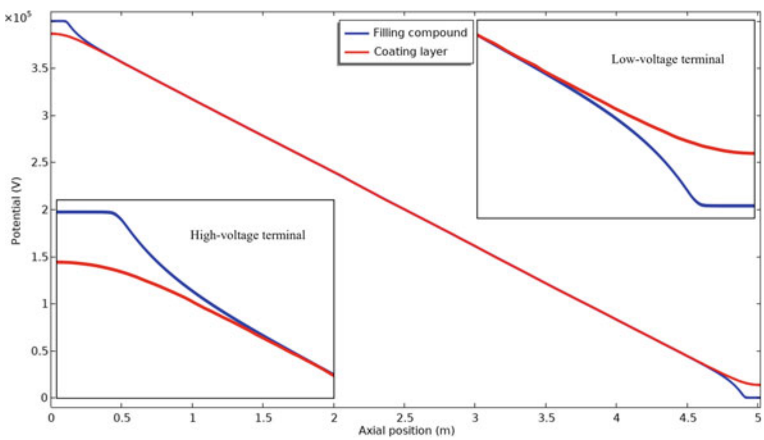


**Fig. 3** The distribution of electric potential along the axial direction

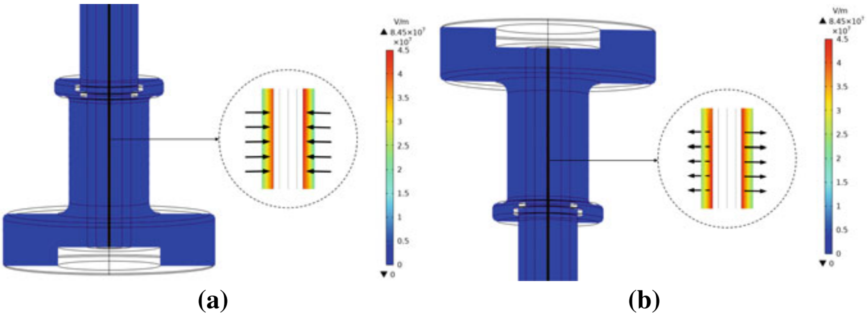


**Fig. 4** Electric field distribution at **a** high-voltage terminal and **b** low-voltage terminal

Figure 4 shows the electric field distribution at high- and low-voltage terminals of the optical fiber insulator, respectively. An electric field distortion occurs in the fiber sheath and the highest electric field strength appears on the inner wall of fiber sheath at interfaces between the fiber sheath and coating layer. The direction of the electric field is dependent on terminals, where the electric fields at the high-voltage and low-voltage terminals are inward and outward, respectively. It is consistent with the calculation results of potentials. The maximum electric field strength in the fiber sheath is up to 84.5 kV/mm. It must be considered that the interfaces between the fiber sheath and coating layer should be taken into account as a critical part due to the large difference in conductivity for the fiber sheath and coating layer, where the order of magnitude is larger than 6.

The electric field for each component along the radial direction passing through the axis in the flange section is shown in Fig. 5. It is apparent that the epoxy tube and filling compound are not subjected to any radial electric field. The highest value of the electric field is localized in the fiber sheath, and the maximum value appears at the interface between the fiber sheath and coating layer. The high peak amplitude of the electric field is above $4 \times 10^7$ V/m. Therefore, the internal discharge mechanism of the optical fiber insulator can be illustrated. The electric field on the inner wall of the fiber sheath in the metal flange section is much larger than that around it, which is easy to trigger a discharge. Meanwhile, the multicomponent interface also can continuously accumulate space charges under the strong radial DC electric field, which will further promote the discharge. In order to further explore the influence of conductivity characteristics of materials on discharges, the changes in electric field distribution with the conductivity of the fiber coating and filling compound are calculated and analyzed.

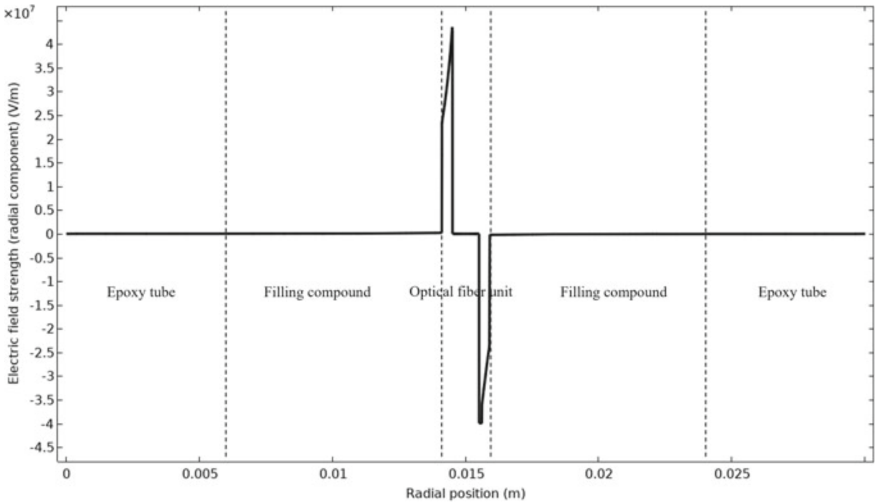


**Fig. 5** Distribution of electric field strength along the radial direction

## 3.2 Variation of Electric Field Distribution with the Conductivity of Coating Layer

Figure 6 exhibits the change in the maximum electric field strength on the fiber sheath with the conductivity of coating layer. The calculation result indicates that the electric field magnitude is strongly dependent on the conductivity of fiber coating layer. When the conductivity ranges from $10^{-14}$ to $10^{-5}$ S/m, the maximum electric field strength varies by up to 4 orders of magnitude. The electric field distortion can be ignored when the conductivity is below $10^{-13}$ S/m. However, the maximum electric field strength sharply enhances as the conductivity increases and the maximum value on the fiber sheath finally reaches a limit value exceeding 1000 kV/mm.

## 3.3 Variation of Electric Field Distribution with the Conductivity of Filling Compound

Besides the fiber coating layer, the effect of the filling compound on the electric field distribution is also needed to be considered because its conductivity is sensitive to moisture. As expected, an electric field distortion is detected on the inner wall of the epoxy tube at the interfaces between the epoxy tube and filling compound, as shown in Fig. 7a. Figure 7b shows the change in the maximum electric field strength on the epoxy tube with the conductivity of filling compound. The result reveals that the electric field magnitude is also highly related to the conductivity of filling compound. The maximum electric field strength varies by around 3 orders of magnitude in the

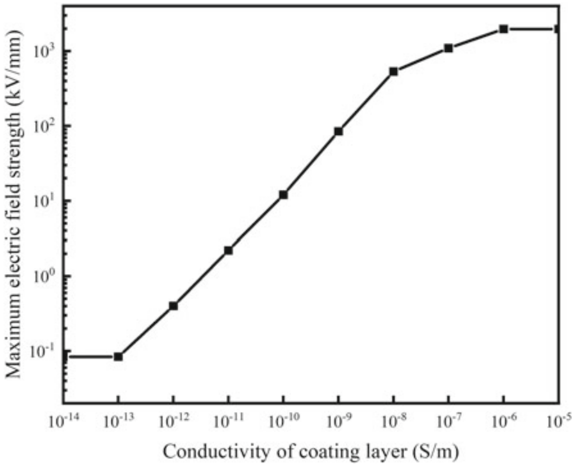


**Fig. 6** The maximum electric field strength on the fiber sheath varies with the conductivity of coating layer

range of $10^{-14}$ to $10^{-6}$ S/m. The electric field distribution is almost uniform when the conductivity is below $10^{-13}$ S/m. Nevertheless, the maximum electric field strength significantly increases as the conductivity increases and the maximum value on the epoxy tube eventually reaches a stable value around 100 kV/mm. Therefore, both conductivities of the fiber coating layer and filling compound are important material characteristics on the electric field distribution. Given conductivities of the fiber coating layer and filling compound, it can be concluded that once the conductivity of the filling compound is higher than that of the coating layer, the electric field distortion in the insulator will be transferred from the fiber sheath to the epoxy tube, as illustrated in Fig. 7b.

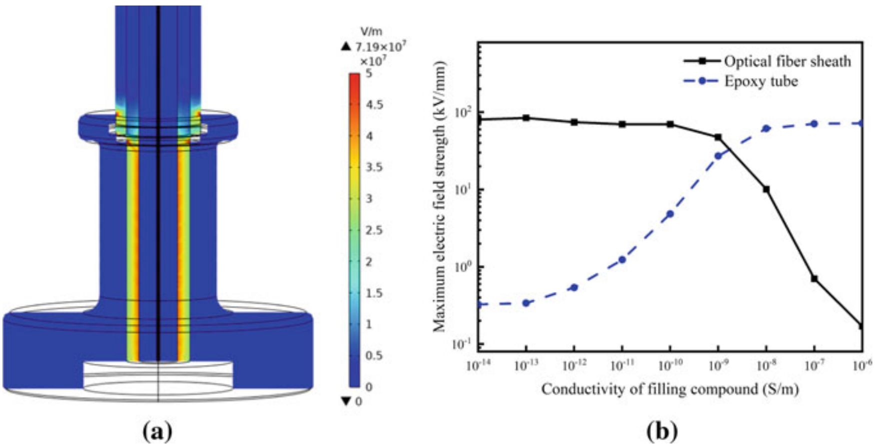


**Fig. 7** **a** Electric field distortion on the inner wall of the epoxy tube and **b** the maximum electric field strength on the fiber sheath and the epoxy tube

## 4 Conclusion

The discharge mechanism of the optical fiber insulator is explored by discussing the effect of material characteristics on the electric field distribution through finite element simulation method. The results show the internal discharge is derived from the obvious electric field distortion at the interfaces between multicomponent in metal flange sections at both high- and low-voltage terminals. The difference in conductivity of internal materials results in mismatched electric potential, which further leads to a radial electric field. Under operating conditions, the electric fields on the inner wall of the fiber sheath and epoxy tube at interfaces can be strongly distorted as the conductivities of fiber coating layer and filling compound increase. Therefore, the conductivity of the materials plays a dominant role in electric field distortion and thus the discharges. It is necessary to keep the conductivity of materials in optical fiber insulators well matched. This work provides a theoretical basis for understanding and preventing the failure of OFCT.

**Acknowledgements** This work was supported by Electric Power Research Institute, CSG EHV Power Transmission Company, Guangzhou (0120002022030301SJ00028). It was also supported by State Key Laboratory of Electrical Insulation and Power Equipment, Xi'an Jiaotong University.

## References

1. Zou C, Wei R, Feng J, Zhou Y (2022) Development status and application prospect of VSC-HVDC. South Power Syst Technol 16(3):1–7
2. Wang C, Chen W, Xu J, Li X, Liu W, Ma J (2022) Analysis of surplus power dissipation strategy of flexible DC transmission system based on energy dissipation resistance. In: 5th International conference on power and energy applications,. IEEE, Guangzhou, China, pp 464–468
3. Wang Q, Huang L, Ying F, Miao Y, Yan J, Liu Y (2021) Topology optimization of offshore DC transmission system based on small signal stability. In: International conference on power system technology. IEEE, Haikou, China, pp 990–994
4. Li Z, Song Q, An F, Zhao B, Yu Z, Zeng R (2021) Review on DC transmission systems for integrating large-scale offshore wind farms. Energy Convers Econ 2(1):1–14
5. Zhao J, Xu S, Wu B, Sun X (2022) Research on the performance of a fiber optical current transformer for high voltage filtering capacitor unbalanced current measurement. J Opt Technol 89(6):353–358
6. Liu C, Zhu X, Su H (2022) Research progress of high sensitivity all fiber optic current sensor. Laser Technology 46(2):175–181
7. Yang X, Zhao Y, Zhang S, Wang Q, Li Q, Chen Z, Liu X, Lu W (2021) Simulation study on inductive characteristics of 800 kV kunliulong DC line. High Voltage Apparatus 57(9):66–71
8. Li J, Zhu B, Guo Y, Liang Z, Wu H, Liu H (2021) The simulation of Kunliulong flexible dc project with single station operation and out of operation. In: Industrial and commercial power system Asia. IEEE, Chengdu, China, pp 1028–1034
9. Shu H, Zhao H, Zhang X, Dong H, Chen N, Bo Z (2021) Reliability analysis of main electrical connection for sending-end converter station in Kunliulong hybrid DC project of China. Autom Electric Power Syst 45(22):115–123

10. Zhou D, Lu Q, Zhou Y, Gu S, Peng W (2021) Multi-terminal DC line fault recovery with fault self-clearing and analysis of converter station online exit strategy. In: 5th Conference on energy internet and energy system integration. IEEE, Taiyuan, China, pp 859–863